

Wavelength Beam Combining for Power and Brightness Scaling of Laser Systems

Antonio Sanchez-Rubio, Tso Yee Fan, Steven J. Augst, Anish K. Goyal, Kevin J.

Creedon, Juliet T. Gopinath, Vincenzo Daneu, Bien Chann, and Robin Huang

Wavelength beam combining allows for scaling the power of a laser system in a modular approach while preserving the quality of the combined beam. Lincoln Laboratory has demonstrated a wavelength-beam-combining technique that significantly improves the brightness and intensity achieved by diode laser systems. This technology could lead to diode lasers' replacing other types of lasers in industrial applications such as metal cutting and welding.



The ideal electric laser efficiently converts electrical power into optical power in the form of a beam that can propagate a long distance with minimal diffraction-limited spreading. Various laser applications require scaling to high power (kW to MW) while maintaining a diffraction-limited beam; thus, many efforts have been directed toward that goal. The main impediment to this high-power scaling has been associated with thermo-optical distortions in the laser gain media that occur as a result of heat generated in the less-than-perfect electrical-to-optical power-conversion process.

For any class of laser, there is a power level that is difficult to exceed without degrading beam quality; however, technological advances have mitigated some thermo-optical effects. For example, diode lasers and fiber lasers are two attractive classes of electric lasers developed to efficiently generate diffraction-limited beams in the W-class and kW-class, respectively. Beam combining offers a modular approach to power scaling while preserving beam quality. The concept of beam combining laser arrays to scale up in power with a diffraction-limited beam is an old one, with some pioneering work done at Lincoln Laboratory in the 1980s [1, 2]. Subsequent laser technology advances have allowed for practical implementations of those beam-combining concepts, and beam combining today is a well-accepted avenue for laser power scaling.

There are two basic approaches for beam combining: coherent and wavelength beam combining. In both approaches, the pointing of each beam needs to be controlled in order to overlap the combined beams. The use of coherent combining in microwaves is well known for radar applications in which tiling of multiple (N) subapertures to increase the total power results in narrowing of the beam in the far field, with a corresponding increase in the far-field on-axis intensity (scales as N^2) on a distant target. This approach requires phase control of the beams from each subaperture of the array. Recent coherent beam combination successfully implemented with lasers is paving the way for practical scaling. The challenge with combining lasers coherently is that, because of their short wavelength, phase control by passive means (i.e., without active sensing and control) has proven to be difficult and has had only limited success. Active means for phase sensing and control have recently allowed for scaling to large-size arrays, including multi-kW demonstrations using fiber laser amplifier arrays [3, 4].

In wavelength beam combining (WBC), a dispersive optical element, such as a diffraction grating, is used to spatially overlap beams of different wavelengths. This technique is similar to wavelength-division multiplexing used in optical communications to increase the number of communication channels that an optical fiber can support. The process of beam combining is the reverse of color separation by a spectrometer. For a given spectral resolution, the number of resolved wavelengths (or beams to be combined) increases as the overall spectral band is increased. In WBC, not only the pointing of each beam but also the wavelength needs to be controlled. WBC is the easier method to accomplish because controlling wavelength is not as challenging as controlling phase, as must be done in coherent beam combining. This article focuses on wavelength beam combining, its potential, and its limitations; comprehensive overviews on beam combining techniques can be found in works by Fan and Yu and Fan [5, 6].

Basic Configurations for Wavelength Beam Combining

The basic methods for WBC are a serial approach and a parallel approach. An example of the serial approach can be found in early work by Nosu, Ishio, and Hashimoto in which band-pass interference filters, one filter

Diffraction-Limited Beam Control

The fundamental optimum resolution of any optical system is limited by diffraction. For example, the resolution d provided by a microscope is given by

$$d = \lambda / (n \sin \theta),$$

where n is the index of refraction for the medium, λ is the wavelength, and θ is the angle subtended by the objective (related to numerical aperture). Similarly, the power of a laser beam that is focused with an angle θ would be concentrated at the focus on a spot of diameter d or larger. A diffraction-limited beam is the one that can be focused down to a spot of size d given by the expression above. To achieve high intensity at the focus, diffraction-limited beams are desirable. Laser beams, or any other form of electromagnetic waves (infrared, microwaves, radio frequencies) will diverge as they propagate according to diffraction rules [a, b].

- a. Wikipedia: http://en.wikipedia.org/wiki/Fraunhofer_diffraction.
- b. Wikipedia: https://en.wikipedia.org/wiki/Fresnel_diffraction

for each wavelength, were used to sequentially add wavelengths [7]. More recently, the serial approach has been implemented using low-loss volume Bragg gratings with narrow spectral width [8]. The serial approach, at least in its basic implementation, requires one separate optical element (a separate combiner) for each wavelength to be combined. In the parallel approach, a single optical element, a diffraction grating, is used to combine multiple beams, each at a different wavelength. The parallel approach is more amenable to scaling to a large number of wavelengths. The work done at Lincoln Laboratory, and the focus of this article, is on the parallel approach.

Closed-Loop Beam Combining

The basic configuration, shown in Figure 1, was used in the first wavelength-beam-combining demonstration of an array of fiber lasers [9]. The key components are an array of gain elements (the diode-pumped fiber amplifiers), a transform optic (lens or mirror), an optical grating (the dispersive element), and a partially reflecting mirror. This mirror serves as the common output coupler for the array of external optical cavities, one cavity for each gain element. For each laser to receive feedback, the laser beam must be normally incident onto the output coupler. As a result, the wavelength of each individual laser is self-determined by its position in the array; its position determines the angle at which the corresponding beam is incident on the grating. The individual beams overlap on the grating and on the output coupler, and they fully overlap as they propagate to the far field. We refer to this configuration as the *closed-loop* combining version.

Diode laser arrays have also been combined using the closed-loop configuration [10, 11]. Diode laser arrays are commonly configured as an array of emitters in a 1 cm wide semiconductor bar. For some applications, the array beams are collimated by a matching microlens array and are propagated to the far field to illuminate a distant object. In the applications of interest in this article, the collimated array beams would be focused by a common lens or mirror to a small spot to achieve high local intensity on a close object.

Wavelength beam combining allows for scaling up not just in power but also in brightness; both power and brightness will scale linearly with the number of elements in the array. Brightness is defined as the power emitted per unit solid angle per unit aperture area, and in the limit when the beam is diffraction limited, it reaches the value P/λ^2 , where P is the power and λ is the wavelength. (See the sidebar entitled “Intensity versus Brightness” for more on these attributes and their role in achieving high local intensity for industrial applications, such as metal cutting and welding.) Figure 2 shows an implementation [11] in which 100 diode laser elements in a 1 cm bar are combined to generate 50 W peak power (pulsed) in a near-diffraction-limited beam.

Open-Loop Wavelength Beam Combining

Another configuration for wavelength beam combining, the open-loop version, is shown in Figure 3. The gain elements are used as amplifiers, in which there is no output coupler to form a laser cavity. The outputs of the amplifi-

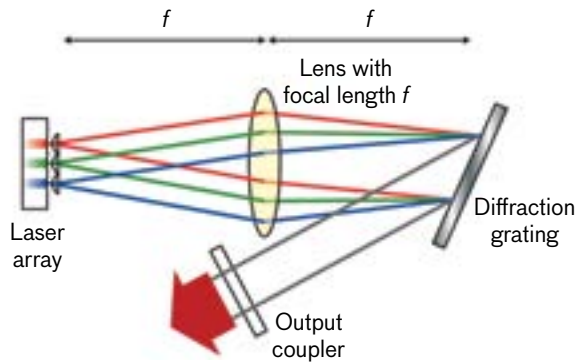


FIGURE 1. Schematic of the beam-combining experiment. Only three lasers are shown for simplicity. A partial reflector—the output coupler—provides feedback to each laser element at a wavelength determined by the angle of incidence on the grating. The far ends of the lasers have a high-reflectivity coating that serves as one end of each of the optical cavities. The laser cavity is thus formed between the high-reflectivity coating and the output coupler’s partial reflector.

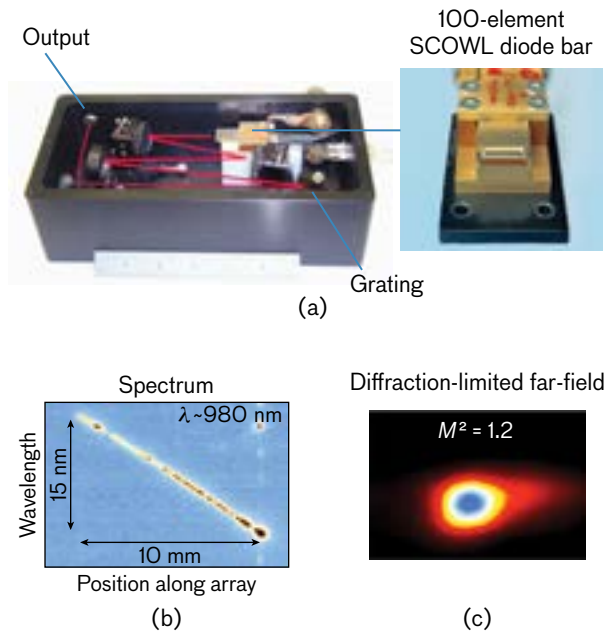


FIGURE 2. (a) Lincoln Laboratory-designed wavelength beam combining (WBC) “laser in a box.” To reduce the overall size of the WBC device, multiple folding mirrors were implemented between the diode array and the concave mirror. The diode array is a bar containing 100 near-diffraction-limited slab-coupled optical waveguide lasers (SCOWL). A 6-inch ruler provides a scale for the size of the box. (b) Spectral measurement shows linear dependence of the wavelength with the position of the element along the array. (c) The quality of the combined beam is near diffraction limited, just as are the individual laser elements.

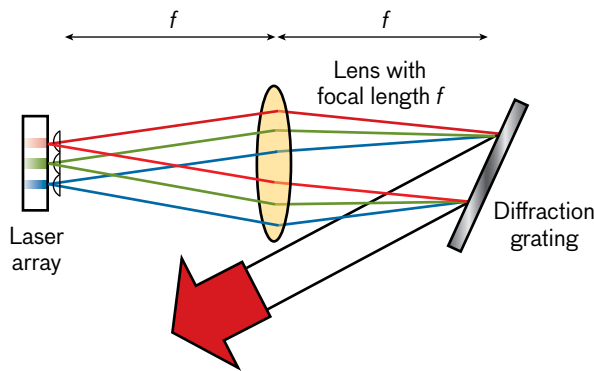


FIGURE 3. Open-loop configuration is shown schematically. The wavelengths of the emitters are adjusted separately and are such that, after diffraction by the grating, the beams overlap in the near and far field.

ers, each amplifier at an appropriate different wavelength, go through the transform optic and are made to overlap on the grating, each beam incident at a different angle. The wavelengths are such that after diffracting from the grating, all the beams fully overlap as they propagate to the far field. Not only do the individual emitters have to be at the correct locations, but their wavelengths also need to be controlled. Open-loop implementations have been performed with fiber amplifier arrays [12] and with diode laser arrays [13]. Diode arrays were wavelength controlled by an external chirped volume Bragg grating that presents feedback at appropriately different wavelengths for different laser elements. In other implementations [14], the wavelength for each element is selected by a grating internal to the laser.

Intensity versus Brightness

Laser cutting and welding of metals require that the intensity of the focused laser beam be sufficiently high so as to raise the temperature and locally melt the metal. A collimated laser beam is characterized by its power P , its beam diameter D (matching the size of the optical aperture), and its angular divergence θ in the far field. It is a well-known fact that as a laser beam is transformed by an optical system, the product $D\theta$ is conserved. Therefore, in going through the focusing optics, the beam is focused down to a spot $d = D\theta/\phi$, where ϕ is the focusing angle. The local **intensity** $I = P/d^2$ can then be expressed as $I = P(\phi/(D\theta))^2 = B\phi^2$, where $B = P/(D\theta)^2$ is defined as the laser beam **brightness**. An optical system with a given focusing angle ϕ will then allow for local intensity proportional to the laser brightness. Brightness (not just power) determines the achievable intensity. Figure A illustrates the geometry of a diverging laser beam with key parameters that define brightness. Figure B illustrates the geometry of a laser being focused to achieve high local intensity.



FIGURE A. Parameters defining the concept of laser brightness. A laser beam with power P and diameter D propagates to the far field with a divergence angle θ . Brightness is defined as $B = P/(D\theta)^2$.

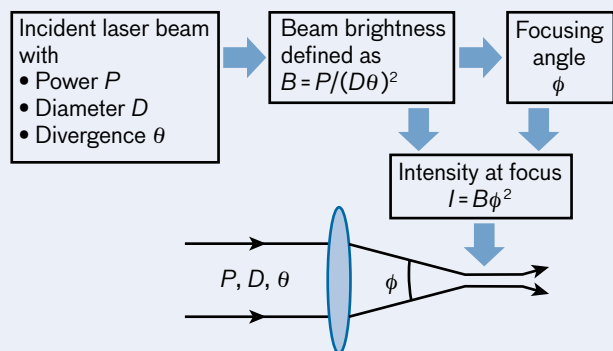


Figure B. Brightness and focusing angle determine intensity at focus. The intensity at the focal spot is given by $I = B\phi^2$, so that for a given focusing angle ϕ , the intensity is proportional to the beam brightness, not just the power.

Limitations on the Number of Elements That Can Be Combined

As we attempt to combine an array with an increasing number of elements, the size of the beam on the grating must also increase due to one (or both) of the following two limiting reasons: (a) the grating resolution must be able to accommodate the larger number of elements, and (b) the optical intensity must remain below a certain critical value so as to avoid optical damage or, perhaps, thermo-optically induced deformations that would degrade the beam quality of the combined beam. At the same time that the beam size increases, the focal length of the transform optic will also change. In this section we will provide scaling rules resulting from these two limitations.

Bandwidth Limitations

The number of beams that can be combined is the ratio of the available global bandwidth to the bandwidth allocated per element. A minimum bandwidth allocation is determined by the dispersive optics used to combine the beams. In order to calculate the maximum allowable number of beams, it is convenient to picture the optics in reverse—as a spectrometer splitting a collimated beam into its wavelength components. Imagine a diffraction-limited beam that contains N wavelengths equally spaced over a band B . The beam is incident on a dispersive optical element (a grating) that splits the beam into its components. For the beams to be separable, the wavelength separation between adjacent beams, $\delta = B/N$, must be such that $\beta\delta \geq \lambda/D$, where β quantifies the optical dispersion and λ/D is the angular divergence of the individual beams. The number of beams that can be combined is then given by $N = \gamma\beta B D/\lambda$, where $\gamma < 1$ is the fill factor (or spectrum utilization factor), which accounts for the angular gap between adjacent beams. In order to combine N wavelengths, the diameter D of the multiwavelength (combined) beam must be $D \geq D_B$, where

$$D_B = N\lambda/(\gamma\beta B).$$

Instead of free-space propagation to reach the far field, a transform lens is used to achieve beam separation in a compact way at the focal plane of the transform optic. (In beam combining, the emitting laser facets would be placed at that plane.) The beam footprint at the focal plane for a single wavelength is $d = f\lambda/D$, the beam separation between adjacent beams is d/γ , and the extent of the foot-

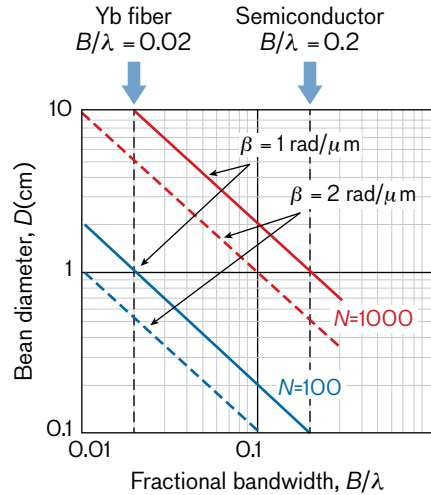


FIGURE 4. Lines of constant number of elements N that can be combined. The horizontal axis is the fractional bandwidth of the spectral envelope. The beam size is on the vertical axis. Two values for the grating dispersion are assumed, $\beta = 1 \text{ rad}/\mu\text{m}$ and $2 \text{ rad}/\mu\text{m}$. The spectral utilization factor is fixed at $\gamma = 0.5$. For operation at $-1 \mu\text{m}$, the vertical dashed lines indicate fractional bandwidths typical of an ytterbium-fiber laser (2%) and a semiconductor-based system (20%) with multiple wavelength-shifted gain media to provide an expanded bandwidth.

print for an array of N wavelengths is Nd/γ . Figure 4 plots lines of constant N where the axes are the fractional bandwidth B/λ in the horizontal axis and the beam diameter D in the vertical axis. Arrays with 100 to 1000 elements, and beyond, can be combined; we could scale up the design for an arbitrarily large number of elements by allowing for sufficiently large values for D and for the global bandwidth B . The need to keep the size of the beam-combining optics within acceptable levels is imposed by practical limits that will be discussed later in the article.

Power and Heat-Dissipation Limitations

Another limitation arises from the need to keep the intensity on the surface of optical components below a critical damage level and below the point at which thermo-optical effects start to introduce significant optical aberrations. In a generic way, if the power per element is P_i and the intensity on any optical component is to be at or below a certain critical value S (assumed to have the same value for each component), then we must design for a beam element size $d \geq (P_i/S)^{1/2}$ and for the combined beam $D \geq D_S = (NP_i/S)^{1/2}$.

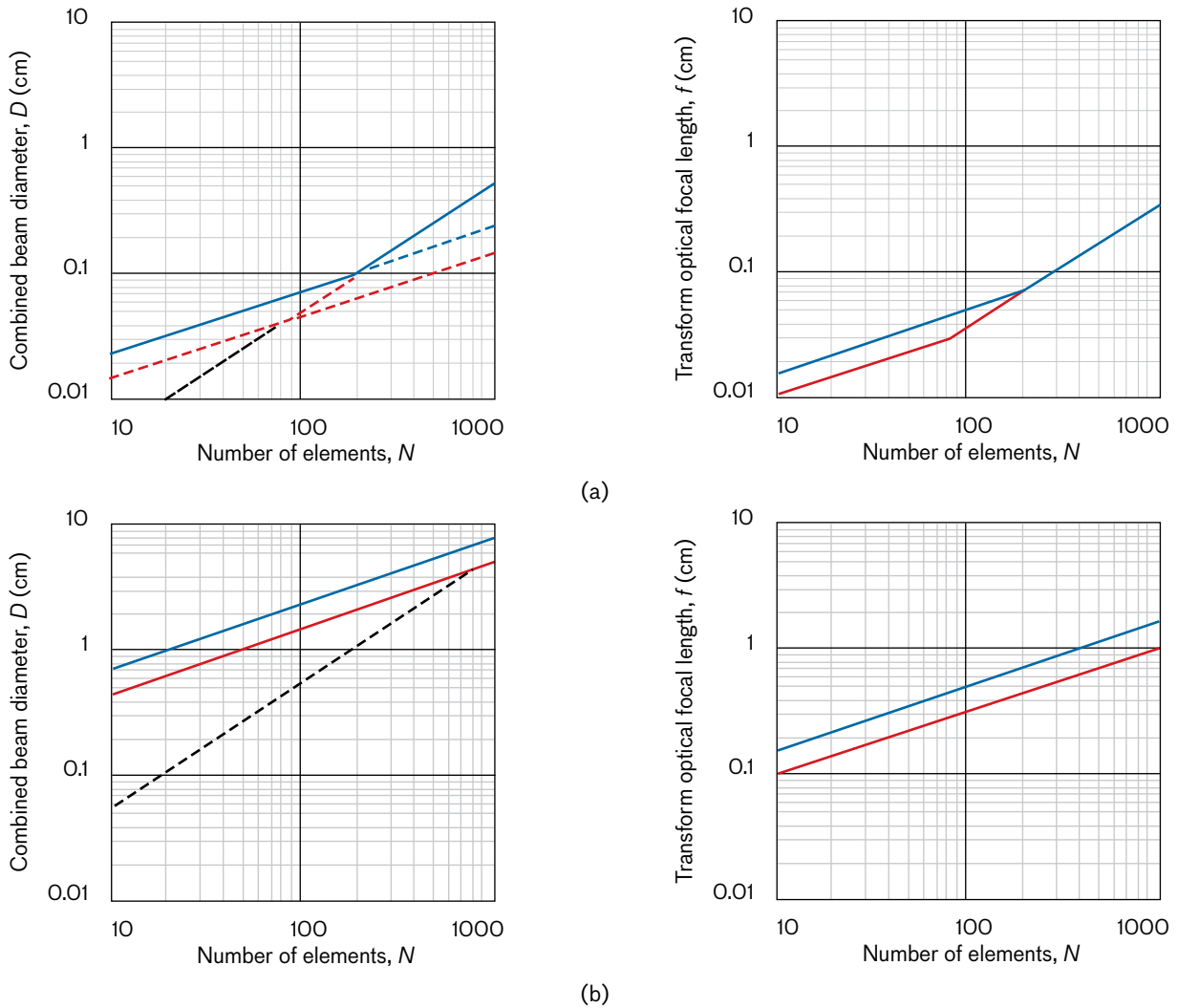


FIGURE 5. The beam size D and the transform optic focal length are plotted versus the number of elements in the array for (a) a semiconductor laser array ($\Delta\lambda = 0.2$, $P_i = 1$ W), and (b) a fiber laser array ($\Delta\lambda = 0.02$, $P_i = 1$ kW). The grating dispersion is assumed to be $\beta = 2$ rad/ μm . Two values are assumed for the critical optical intensity S (20 kW/cm² in blue and 50 kW/cm² in red). Note the transition from D and f scaling as $N^{1/2}$ (intensity-limited regime) to D and f scaling as N (bandwidth-limited regime). A design for combining a semiconductor laser array of 1000 elements would be bandwidth limited, and it would require an output beam $D \geq 0.5$ cm and $f \geq 40$ cm.

In designing a combiner for N elements, we must then select the optics such that the combined beam diameter is, at least, the larger of D_S and D_B [$D > D_S, D_B$]. The focal length of the transform optic is then given by $f = D d / \lambda$. If $D_B > D_S$ (bandwidth-limited design), the focal length is

$$f > f_B = (P_i / S)^{1/2} N / (\gamma \beta B).$$

If $D_S > D_B$ (intensity-limited design), the focal length is

$$f > f_S = N^{1/2} P_i / (S \lambda).$$

Figure 5 shows the results for two generic examples: a semiconductor laser array ($B/\lambda = 0.2$, $P_i = 1$ W) and a fiber laser array ($B/\lambda = 0.02$, $P_i = 1$ kW). Two values for the critical intensity S are assumed: 20 and 50 kW/cm². (These values are intended to be representative of limiting intensities for high-performance optical gratings.) As the array size N increases, the beam diameter D is initially determined by the limiting intensity S and scales as $N^{1/2}$; at some critical value of $N = N_c = (\gamma \beta B / \lambda)^{1/2} P_i / S$, there is a transition to being limited by the spectral resolution (bandwidth limit), and in this regime D scales as N . There is a corresponding behav-

ior for the focal length of the transform optic, $f = Dd/\lambda$. It can be observed in Figure 5 that the focal length for combining a diode laser array with 300 elements is 10 cm and it is bandwidth limited. On the other hand, combining 300 fibers would be intensity limited, and it would require a focal length ranging from 55 m (for $S = 50 \text{ kW/cm}^2$) to 90 m (for $S = 20 \text{ kW/cm}^2$). These long focal lengths would make the system impractically large if it were to be implemented with a single lens or mirror. It is possible to design a compact transform optical system with multiple optical elements while keeping the intensity on all optical elements below the critical value. Details for such a point design of the optics are beyond the scope of this article.

An alternate design option makes use of cylindrical rather than spherical optics and leads to quite smaller values of the focal length. A cylindrical lens focuses a beam to a line (in one dimension), in contrast to a spherical lens that focuses it to a point (in two dimensions), to a much higher intensity for the same focal length. With cylindrical optics, it would be $d = P_i^{1/2}/(NS)^{1/2}$, $f_B = (NP_i/S)^{1/2}/(\gamma\beta B)$, and $f_S = P_i/(S\lambda)$. Table 1 lists, for comparison, the expressions for d , D , and f when using spherical and cylindrical optics. Note that the value of the focal length (and d) scales less dramatically with N when using cylindrical optics; compared to the case of spherical optics, the focal length is reduced by a factor $N^{-1/2}$. Cylindrical optics are generally more challenging to fabricate, so that their use would appear to be attractive only if they provide significant packaging advantages.

Dispersive Element – the Diffraction Grating

Critical among the various optical elements is the dispersive element (in our case, a grating). The number of elements that can be combined for a given beam diameter D and global bandwidth B is proportional to the magnitude of the grating dispersion β . The choice of grating determines the dispersion. The grating needs to efficiently diffract into the desired order, and it needs to withstand the high incident optical intensity without distorting the diffracted beam. Fortunately, dielectric gratings have been fabricated with 96% diffraction efficiency [15, 16], and with absorption losses of $<10^{-4}$, they can accept high intensity with negligible thermo-optical distortions.

Grating Geometry

A beam incident on a grating at an angle α relative to the grating normal generates, in general, multiple diffracted-order beams, one for each order m . The diffraction angle θ_m for the m th order beam is governed by the grating equation

$$d (\sin \alpha + \sin \theta_m) = m\lambda ,$$

where d is the grating period (see Figure 6). We will assume that the grating profile is such that most of the incident power is diffracted into the desired m order. We will also assume that at the nominal center wavelength λ_0 , of the band to be combined, the diffracted beam is at an angle θ_m that is at or near the angle of incidence,

Table 1. Scaling with Number N for d , D , and f When Using Spherical and Cylindrical Optics		
	SPHERICAL	CYLINDRICAL
d	$(P_i/S)^{1/2}$	$P_i^{1/2}/(NS)^{1/2}$
D_B	$N\lambda/(\gamma\beta B)$	$N\lambda/(\gamma\beta B)$
D_S	$(NP_i/S)^{1/2}$	$(NP_i/S)^{1/2}$
f_B	$(P_i/S)^{1/2} N/(\gamma\beta B)$	$(NP_i/S)^{1/2}/(\gamma\beta B)$
f_S	$N^{1/2} P_i/(S\lambda)$	$P_i/(S\lambda)$
The values for D_B and D_S are the same in both columns. The smaller value, by $N^{1/2}$, for d in the cylindrical case carries through to smaller values for f_B and f_S .		

α_m , called the Littrow condition, $\theta_m \sim \alpha_m$, illustrated in Figure 6. This condition is satisfied by selecting a grating period, $d = d_m$ such that $2d_m \sin \alpha_m = m \lambda_0$. The magnitude of the dispersion, $\beta = \delta\theta_m/\delta\lambda$, quantifies the change in the diffracted angle for a small change in the wavelength. Under these conditions, the dispersion is given by

$$\beta = (2/\lambda_0) \tan \alpha_m,$$

and we can select the value of α_m for a desired dispersion β :

$$\alpha_m = \tan^{-1}(\beta\lambda_0/2).$$

Table 2 shows examples for three desired values of β . Included are the corresponding values for the grating period d for $m = 1$, assuming a nominal $\lambda_0 = 1 \mu\text{m}$.

All these cases satisfy $\alpha > 19.5$ degrees (or $\sin \alpha > 1/3$), the condition to ensure that the only allowed diffracted orders are the first and the zeroth order. Designing for $m > 1$ will necessarily result in additional diffraction orders. Because subsequent beam-combining efficiency is mostly determined by losses at the grating caused by unwanted diffraction orders, it is most convenient to employ gratings that support only first and zeroth orders. It is possible to design gratings where, at the center wavelength and for a specific polarization, only <1% of the incident power is lost in the zeroth order. Furthermore, the use of dielectric coatings on the grating (in contrast to metal coatings) results in very little absorption ($<10^{-4}$), leading to the potential for high combining efficiency. An important additional benefit of using dielectric gratings (compared to metal-coated gratings) is that the thermal load is very low, resulting in greatly reduced thermo-optical distortions.

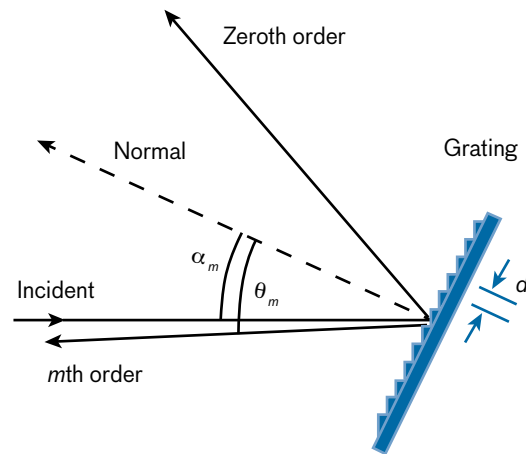


FIGURE 6. Grating geometry in the near-Littrow condition. The diffracted beam satisfies $\theta_m \sim \alpha_m$, and most of the diffracted power is in the m th order. The residual zeroth order reflection is shown by the faint line.

Wavelength Beam Combining a Two-Dimensional Laser Amplifier Array

So far, this article has considered the case in which a single dispersive element (i.e., a grating) is used to separate (or combine) the wavelengths. The array of elements is one-dimensional. There may be cases in which the number of elements is large enough and the spacing between elements large enough that a two-dimensional (2D) array would be attractive and lead to a more compact package. In order to accommodate a 2D array of emitters, a 2D optical disperser would be needed.

Our design for beam combining in two dimensions uses cylindrical optics. As mentioned earlier, cylindrical optics lead to designs with shorter focal length than the focal length used by spherical optics. This benefit would, however, come at a cost in fabrication difficulty; it could

Table 2. Grating Period and Angle of Incidence to Achieve $\beta = 1, 2,$ and $4 \text{ rad}/\mu\text{m}$		
DISPERSION $\beta \text{ (rad}/\mu\text{m})$	ANGLE OF INCIDENCE $\alpha \text{ (degrees)}$	GRATING PERIOD $d \text{ (}\mu\text{m)}$
1	26.5	1.118
2	45	0.7071
4	63.4	0.5590
The center wavelength is $\lambda_0 = 1 \mu\text{m}$.		

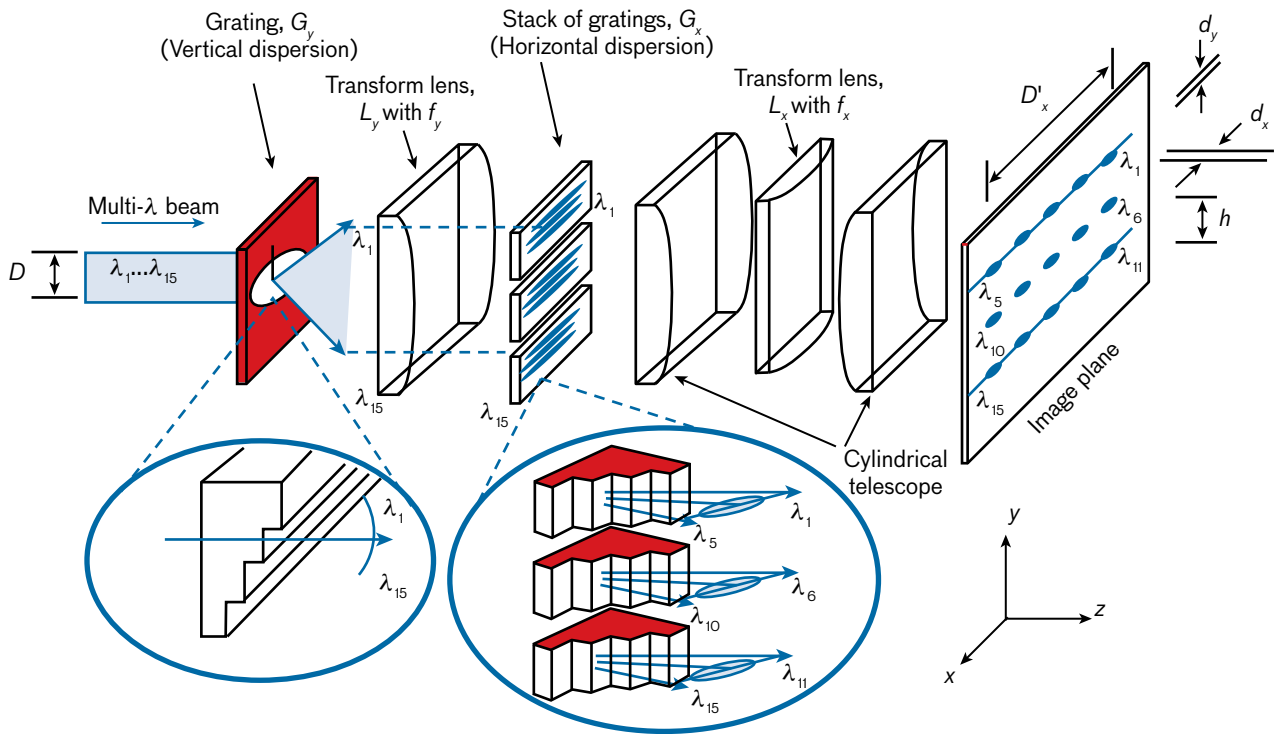


FIGURE 7. Concept for two-dimensional wavelength beam combining. The optical layout shows the crossed gratings (the single vertical grating and the stack of horizontal dispersion gratings). The cylindrical transform lens f_y focuses the multi-wavelength beam (coming from the left) to a series of horizontal lines, one for each wavelength. After one of the beams is incident on one of the gratings in the stack, the beam pointing in the horizontal plane changes with wavelength. The transform lens f_x , together with the cylindrical relay telescope, brings the beam to a focus in the image plane. Each grating in the stack has an appropriately different dispersion value; as the wavelength changes and the beam transitions for the top grating to the next in the stack, a new line is initiated in the image plane. Each grating in the stack covers a spectral subrange, and there is a corresponding line in the image plane. For clarity in visualization, the example in the figure shows three gratings and five wavelengths per grating.

also be anticipated that the need for a second disperser (see Figure 7) would result in additional combining efficiency loss. (For the mathematics behind Figures 7 and 8, see the appendix of this article.) It is worth highlighting that the two-dimensional grid supporting the location of the emitters will not be in the form of a series of perfectly straight lines because of the difference in nonlinear wavelength dependence of the diffracted angle in two dimensions (the dispersion β is just a linear approximation, valid over a limited range of wavelengths). The distortion of such a grid, as small as it is, needs to be anticipated in the design so that the emitters are correctly placed within a small fraction of their beam diameters in order to maintain good beam overlap of the components at the combined beam. Imperfect overlap would lead to a decrease in the far-field on-axis intensity of the combined beam, equivalent to a reduction in beam-combining efficiency. With emitters

placed at their correct location, a closed-loop configuration with a common output coupler to feed back the combined beam would automatically determine the wavelength of each emitter, just as in the one-dimensional closed-loop case. In the open-loop configuration, the wavelengths of individual emitters would also need to be precisely controlled, just as in the one-dimensional case.

In scaling up the number of elements to be combined, at some point there is a role for two-dimensional beam combining. Exactly where that point lies depends on a careful comparison of one-dimensional and 2D point designs. The objective is to disperse a multiwavelength beam into its spectral components, forming a 2D pattern. Used in reverse, "assembling" the beams provides a method for 2D WBC. Figure 7 shows a multiwavelength, diffraction-limited beam with diameter D and spectrum spread over a bandwidth B that is incident from the left on a grating G_y .

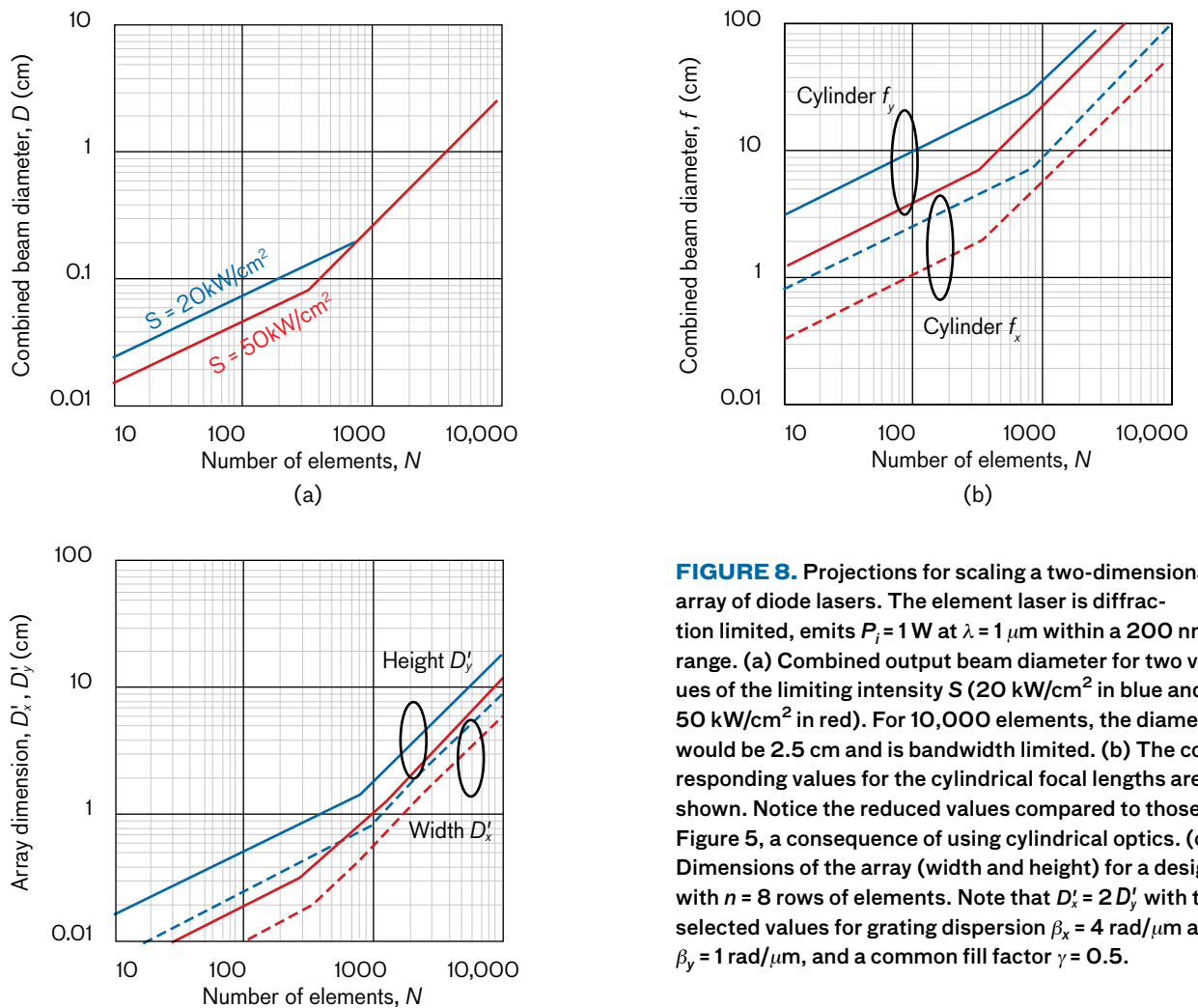


FIGURE 8. Projections for scaling a two-dimensional array of diode lasers. The element laser is diffraction limited, emits $P_e = 1 \text{ W}$ at $\lambda = 1 \mu\text{m}$ within a 200 nm range. (a) Combined output beam diameter for two values of the limiting intensity S (20 kW/cm^2 in blue and 50 kW/cm^2 in red). For 10,000 elements, the diameter would be 2.5 cm and is bandwidth limited. (b) The corresponding values for the cylindrical focal lengths are shown. Notice the reduced values compared to those in Figure 5, a consequence of using cylindrical optics. (c) Dimensions of the array (width and height) for a design with $n = 8$ rows of elements. Note that $D'_x = 2 D'_y$ with the selected values for grating dispersion $\beta_x = 4 \text{ rad}/\mu\text{m}$ and $\beta_y = 1 \text{ rad}/\mu\text{m}$, and a common fill factor $\gamma = 0.5$.

The design task will specify the optical components—grating and lenses—in order to combine N elements that are placed in a 2D pattern with n rows. Figure 8 shows specific results for an example in which a 2D array of diode lasers is combined. The output beam diameter D values for the two focal lengths f_x and f_y , and the dimensions D'_x, D'_y , of the 2D diode array are plotted versus the number N of array elements for an array with $n = 8$ rows.

Emitter Element Spectrum and Quality of Combined Beam

So far it has been assumed that the emitter element spectrum is very narrow. Each emitter with a wavelength within the global band B is assigned a location in the Fourier plane. Its emission propagates through the combining optics and exits, filling the output aperture and pointing in a direction that is common for all emitters. Also pre-

sented has been how to design for a large number of elements. With emitter beams that are diffraction limited, the combined beam will also be diffraction limited. As the number N of elements increases—as the bandwidth allocation B/N per element decreases—there is a point at which the spectral linewidth of the emitter element may no longer be narrow enough and, consequently, its spectral content gives rise, when dispersed by the grating, to a far field that is no longer diffraction limited.

Let us consider the example in which the bandwidth allocation per element is 10 GHz . This allocation would allow us to combine up to 600 elements within $B = 20 \text{ nm}$ global bandwidth ($10 \text{ GHz} \sim 0.033 \text{ nm}$ at $1 \mu\text{m}$). Fiber laser amplifiers have demonstrated 1 kW within a 10 GHz linewidth. An array of 600 such elements would produce a 600 kW beam; such a beam, however would be approximately twice diffraction limited (at best, for fill factor $\gamma \sim 1$). There

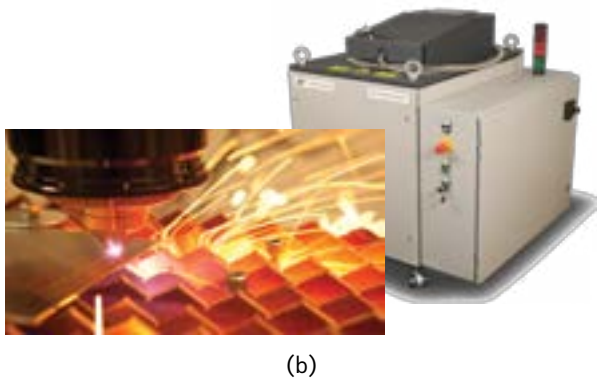
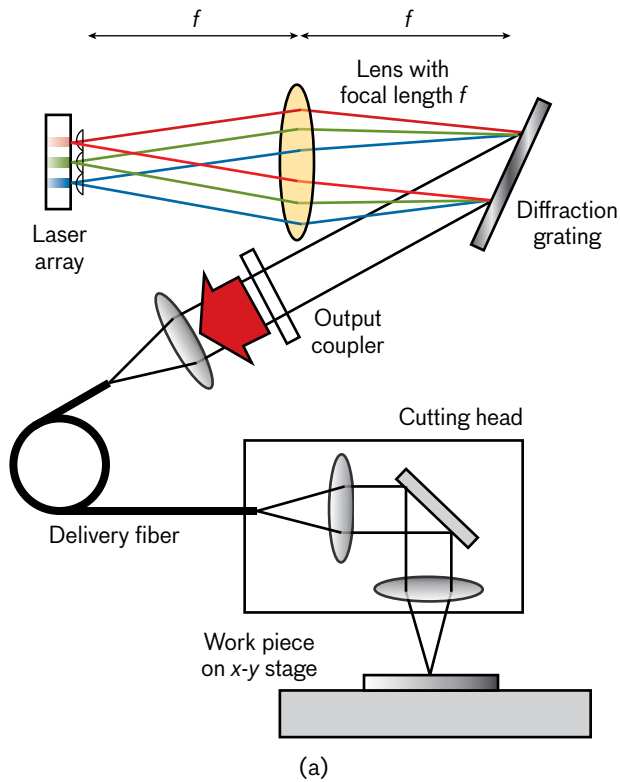


FIGURE 9. Transfer of WBC technology to TeraDiode. (a) Schematic of the direct-diode cutting system. (b) The processing head is shown cutting through 0.26-inch steel. The WBC beam is coupled to a 100 μm /0.1 numerical-aperture fiber to output 2 kW continuous-wave power. The laser system in the background shows the coiled delivery fiber that would connect to the processing head.

are techniques to “precompensate” for the effects of finite element bandwidth by arranging, with additional optics, for each spectral component within a beam element to be incident on the grating at an appropriately different angle. With such a precompensation technique [17], the deleterious effects can be greatly mitigated.

Industrial Applications of Beam-Combined Diode Lasers to Cutting and Welding

Multi-kilowatt-class lasers are used in cutting, welding, and other industrial applications in which the high-intensity laser beam is used to locally raise the temperature of the material. These kW-class lasers include CO₂, fiber, bulk solid-state, and disk lasers. In the past, individual diode lasers, while having a number of attractive features (they are compact, low-cost, reliable, and wavelength-versatile), were limited in power and brightness. Individual diode lasers are limited in power to the ~1 W class for diffraction-limited beams, and conventional diode laser arrays without beam combining do not provide beams with the required brightness.

Wavelength beam combining of arrays of diode lasers is an alternate approach to produce kW-class lasers with sufficient beam quality (and brightness) to cut and weld metals. This direct-diode approach, based on technology developed at Lincoln Laboratory, has recently been commercialized and demonstrated at the kW level by TeraDiode, Inc. [18]. This approach has the potential to bring about the replacement of current industrial lasers with lower-cost diode lasers for use in a variety of manufacturing applications.

TeraDiode developed the first direct-diode lasers that are bright enough to cut and weld metal. Their 2 kW laser system cutting head can cut through 0.26-inch steel plate (Figure 9). The laser is housed in a stainless steel enclosure. The system includes the chiller and plumbing manifold, control computer, power supplies, power conditioning and distribution unit, and emergency stop switch. The laser output is coupled to a 100 μm diameter core processing fiber, which has end connectors compatible with industrial fiber connectors. The output end of the fiber is coupled to a processing head that can be configured for cutting or welding. WBC technology enables diode lasers to achieve the power and brightness required to perform the functions of current industrial lasers. Direct-diode lasers using WBC technology may, in time, replace fiber, disk, and other lasers for demanding material-processing applications.

Future Directions

Fiber lasers and diode lasers, operating at $\sim 1 \mu\text{m}$, have high efficiency and can operate over a large spectral bandwidth. Those two attributes make them very attractive as building blocks for high-power WBC lasers. Other spectral bands could be accessed with different types of lasers as long as they are efficient and provide large gain bandwidth. Quantum cascade lasers and parametric frequency conversion using nonlinear optics are two avenues for developing WBC systems in the midwave and longwave infrared ranges. For example, a 25-element array with emission spanning over 1.44 to 1.46 μm has been wavelength beam combined [19] to generate 20 W in a near-diffraction-limited beam, and an array of quantum cascade lasers has been wavelength beam combined [14] to provide a multiwavelength (8.73 to 9.42 μm), near-diffraction-limited beam.

While the main focus in this article has been on WBC technology for enabling scaling to high-power and high-brightness lasers, other modes of operation may enable other applications in the future. With individual addressability, it would be possible to operate only a subset of lasers (or one laser at a time); such spectral agility could enable novel uses (e.g., wavelength tailoring for various spectroscopic sensing applications). For remote sensing applications, the spectral emission profile can be rapidly changed. This capability could also apply to optical (or infrared) laser communications with wavelength diversity. ■

References

1. J.R. Leger, M. Holz, G.J. Swanson, and W.B. Veldkamp, "Coherent Laser Beam Addition: An Application of Binary-Optics Technology," *Lincoln Laboratory Journal*, vol. 1, no. 2, 1988, pp. 225–246.
2. Z.L. Liao, V. Diadiuk, and J.N. Walpole, "Microlens Integration with Diode Lasers and Coherent Phase Locking of Laser Arrays," *Lincoln Laboratory Journal*, vol. 3, no. 3, 1990, pp. 385–394.
3. S.M. Redmond, D.J. Ripin, C.X. Yu, S.J. Augst, T.Y. Fan, P.A. Thielen, J.E. Rothenberg, and G.D. Goodno, "Diffraction Coherent Combining of a 2.5 kW Fiber Laser Array into a 1.9 kW Gaussian Beam," *Optics Letters*, vol. 37, no. 14, 2012, pp. 2832–2834.
4. C.X. Yu, S.J. Augst, S.M. Redmond, K.C. Goldizen, D.V. Murphy, A. Sanchez-Rubio, and T.Y. Fan, "Coherent Combining of a 4 kW, Eight-Element Fiber Amplifier Array," *Optics Letters*, vol. 36, no. 14, 2011, pp. 2686–2688.
5. T.Y. Fan, "Laser Beam Combining for High-Power, High-Radiance Sources," *IEEE Journal of Selected Topics in Quantum Electronics*, vol. 11, no. 3, 2005, pp. 567–577.
6. C.X. Yu and T.Y. Fan, "Beam Combining," in *High Power Laser Handbook*, New York: McGraw Hill, 2011.
7. K. Nosu, H. Ishio, and K. Hashimoto, "Multireflection Optical Multi/Demultiplexer Using Interference Filters," *Electronics Letters*, vol. 15, no. 14, 1979, pp. 414–415.
8. A. Sevian, O. Andrusyak, I. Ciapurin, V. Smirnov, G. Venus, and L. Glebov, "Efficient Power Scaling of Laser Radiation by Spectral Beam Combining," *Optics Letters*, vol. 33, no. 4, 2008, pp. 384–386.
9. C.C. Cook and T.Y. Fan, "Spectral Beam Combining of Yb-Doped Fiber Lasers in an External Cavity," OSA Trends in Optics and Photonics Series, vol. 26, *Advanced Solid State Lasers*, M.M. Fejer, H. Injeyan, and U. Keller, eds. Washington, D.C.: Optical Society of America, 1999.
10. V. Daneu, A. Sanchez, T.Y. Fan, H.K. Choi, G.W. Turner, and C.C. Cook, "Spectral Beam Combining of a Broad-Stripe Diode Laser Array in an External Cavity," *Optics Letters*, vol. 25, no. 6, 2000, pp. 405–407.
11. R.K. Huang, B. Chann, L.J. Missaggia, J.P. Donnelly, C.T. Harris, G.W. Turner, A.K. Goyal, T.Y. Fan, and A. Sanchez-Rubio, "High-Brightness Wavelength Beam Combined Semiconductor Laser Diode Arrays," *IEEE Photonics Technology Letters*, vol. 19, no. 4, 2007, pp. 209–211.
12. S.J. Augst, A.K. Goyal, R.L. Aggarwal, T.Y. Fan, and A. Sanchez, "Wavelength Beam Combining of Ytterbium Fiber Lasers," *Optics Letters*, vol. 28, no. 5, 2003, pp. 331–333.
13. B. Chann, A.K. Goyal, T.Y. Fan, A. Sanchez-Rubio, B.L. Volodin, and V.S. Ban, "Efficient, High-Brightness Wavelength-Beam-Combined Commercial off-the-Shelf Diode Stacks Achieved by Use of a Wavelength-Chirped Volume Bragg Grating," *Optics Letters*, vol. 31, no. 9, 2006, pp. 1253–1255.
14. B.G. Lee, J. Kinsky, A.K. Goyal, C. Pflugl, L. Diehl, M.A. Belkin, A. Sanchez, and F. Capasso, "Beam Combining of Quantum Cascade Laser Arrays," *Optics Express*, vol. 17, no. 18, 2009, pp. 16216–16224.
15. J.A. Britten, S.J. Bryan, L.J. Summers, H.T. Nguyen, B.W. Shore, and O. Lyngnes, "Large Aperture, High-Efficiency Multilayer Dielectric Reflection Gratings," *Technical Digest of the Summaries of Papers Presented at the IEEE Conference on Lasers and Electro-Optics*, 2002, pp. CPDB7-1–CPDB7-4.
16. N. Destouches, A.V. Tischenko, J.C. Pommier, S. Reynaud, O. Parriaux, S. Tonchev, and M. Abdou Ahmed, "99% Efficiency Measured in the -1st Order of a Resonant Grating," *Optics Express*, vol. 13, no. 9, 2005, pp. 3230–3235.
17. E.C. Cheung, J.G. Ho, T.S. McComb, and S. Palese, "High Density Spectral Beam Combination with Spatial Chirp Pre-compensation," *Optics Express*, vol. 19, no. 21, 2011, pp. 20984–20990.
18. R.K. Huang, B. Chann, and J.D. Glenn, "Ultra-High Brightness, Wavelength-Stabilized, kW-Class Fiber-Coupled Diode Laser," *Proceedings of SPIE*, vol. 7918, 2011, pp. 791810-1–791810-9.
19. J.T. Gopinath, B. Chann, T.Y. Fan, and A. Sanchez-Rubio, "1450-nm High-Brightness Wavelength-Beam Combined Diode Laser Array," *Optics Express*, vol. 16, no. 13, 2008, pp. 9405–9410.

Appendix

Two-Dimensional Wavelength Beam Combining of Lasers

Consider a diffraction-limited beam with diameter D and spectrum spread over a bandwidth B that is incident on a grating G_y . The beam is dispersed over an angle $\beta_y B$ in the vertical (y - z) plane, where β_y is the average dispersion over the wavelength range (bandwidth) B . A cylindrical lens L_y with focal length f_y maps each spectral component at its Fourier plane into a linear footprint of width $w = f_y \lambda/D$, and the footprint of all the spectral components spreads over $\beta_y B f_y$. At the Fourier plane of L_y , there is a stack with n gratings to disperse each component beam in the horizontal (x - z) plane. Each grating has a height $h = \beta_y \Delta f_y$ so as to intercept components within a bandwidth $\Delta = B/n$. The period d or the angle of incidence α for grating k of the stack ($1 < k < n$, counting from the top) is such that the diffracted beam for $\lambda_k = \lambda_0 + (k - 1/2) \Delta$ —incident on the mid-height level of k -grating—is along the nominal optical axis. For a range of wavelengths Δ centered at λ_k , that is for $\lambda_k - \Delta/2 < \lambda < \lambda_k + \Delta/2$, the diffracted beam is off axis, at angle $\beta_{x,k} (\lambda - \lambda_k)$ in the horizontal (x - z) plane. A lens L_x with focal length f_x , together with a cylindrical relay telescope with unity magnification, transforms the beam with wavelength λ to a spot with dimensions

$$d_x = \lambda f_x / D$$

and

$$d_y = \lambda f_y / D$$

at location in the image plane given by

$$x = \beta_{x,k} (\lambda - \lambda_k) f_x$$

and

$$y = \beta_{y,k} (\lambda - \lambda_k) f_y.$$

As the wavelength changes from λ_0 to $\lambda_0 + B$, the beam is mapped to a set of $N_y = B/\Delta$ lines, similar to a raster scan. The number of elements in line k of the scan is given by

$$N_x = \gamma \beta_{x,k} \Delta D / \lambda$$

and are spread over a length $D'_x = \beta_{x,k} \Delta f_x$ with a spatial fill factor given by γ .

The spacing between lines is $h_k = \beta_{y,k} \Delta f_y$ so that $N_y = B/\Delta$ lines extend over $D'_y = \beta_{y,k} B f_y$ where $\beta_y = \langle \beta_{y,k} \rangle$ is the average dispersion for grating G_y over the wavelength range B . The total number of combined elements is

$$N = N_x N_y = \gamma \beta_x B D / \lambda,$$

where β_x is the average dispersion for the grating stack over the wavelength range B . Note that this is the same expression as for the linear array, the basis for the plots in Figure 5. In the 2D concept, the same number N of elements will now be distributed in $n = N_y$ rows.

The design task will specify the optical components—grating and lenses—in order to combine N elements in a 2D pattern with n rows of elements. The total available bandwidth B is given. The element is specified by its power P_i and beam diameters d_x and d_y , consistent with not exceeding a critical optical intensity S ,

$$d_x = d/r, d_y = d r$$

and

$$r^2 = d_y / d_x,$$

where $d = (P_i/S)^{1/2}$ and r^2 is the element beam aspect ratio. The combined beam diameter D must be large enough to satisfy the critical intensity condition

$$D > D_S = (N P_i / S)^{1/2},$$

and it must also be large enough to provide angular separation of adjacent dispersed beams with dispersion β_x and spatial fill factor γ so that

$$D > D_B = \lambda N / (\gamma \beta_x B).$$

It follows that the focal lengths are then given by

$$f_x = d_x D / \lambda$$

and

$$f_y = d_y D / \lambda.$$

The length D'_x of one row is given by

$$D'_x = \beta_x \Delta f_x,$$

where $\Delta = B/n$ is the bandwidth allocation per row. The vertical extent of the n rows in the 2D layout is then given by

$$D'_y = \beta_y B f_y,$$

where the dispersion β_y is selected at this point consistent with a desired value for D'_y (a desired value for inter-row spacing $h = D'_y/n$). It is interesting to note the following relationship

$$D'_y / D'_x = (\beta_y / \beta_x)(d_y/d_x) n$$

that links the number of rows n to the ratios of other design parameters. If we were to impose that $D'_x = D'_y$ and $d_x = d_y$, the ratio of the dispersion values must then be selected to match the number of rows $n = \beta_x/\beta_y$. The dispersion β_y in the vertical dimension must then be slow compared to the dispersion β_x in the horizontal.

About the Authors



Antonio Sanchez-Rubio is a senior staff member in the Laser Technology and Applications Group at Lincoln Laboratory. His research interests are in laser development and in the use of lasers to sensing applications. He has made contributions in the areas of semiconductor lasers and diode-pumped solid-state lasers. He has worked on the development of laser systems and sensors for laser radar, infrared countermeasures, and bioaerosol detection. He has contributed to the development of laser beam-combining techniques for power and brightness scaling using semiconductor laser arrays and fiber laser arrays. His current work is focused on laser beam combining and on quantum-cascade lasers for spectroscopic sensing applications in the mid- and long-wave infrared. He has more than 40 publications in refereed journals and is a coinventor on 5 patents. He is the corecipient of the 2012 Berthold Leibinger Innovationspreis (First Prize). He received a bachelor's degree in physics from the Universidad Complutense of Madrid, Spain, and a doctoral degree in physics from the Massachusetts Institute of Technology.



Tso Yee (T. Y.) Fan is the associate leader of the Laser Technology and Applications Group at Lincoln Laboratory. He joined the Laboratory in 1987. He is widely recognized in the laser community for his pioneering work in diode-pumped solid-state lasers, in advances in cryogenic lasers for improving average-power scalability, in characterization of laser and nonlinear optical materials, and in advances in laser beam combining. Dr. Fan is a Fellow of the Optical Society of America and a senior member of the Institute of Electrical and Electronics Engineers. He served as an elected member of the IEEE/LEOS Board of Governors from 1994–1996 and was the topical editor, lasers, for *Optics Letters* from 1994–1999. He received the 2009 MIT Lincoln Laboratory Technical Excellence Award for his work on Yb lasers, cryogenic lasers, and laser beam combining, and the 2011 MIT Lincoln Laboratory Best Invention Award. He is a corecipient of the 2012 Berthold Leibinger Innovationspreis (First Prize). He received bachelor's degrees in electrical engineering and materials science and engineering from the Massachusetts Institute of Technology and master's and doctoral degrees in electrical engineering from Stanford University.



Steven J. Augst is a staff member in the Laser Technology and Applications Group. Since joining Lincoln Laboratory in 2001, he has led a number of projects to develop spectral and coherent beam-combining techniques to scale laser systems to high power in a modular fashion. He also frequently serves as a technical advisor to the

government for several programs that involve high-power laser development by defense contractors. Prior to joining the Laboratory, he worked at the California Institute of Technology to develop interferometric-based gravitational-wave detectors, and at Imperial College, London, to develop ultrashort-pulse laser systems. He holds a doctoral degree in physics from the University of Rochester, where his research focused on the interaction of atoms with extreme electrical fields generated by short-pulse lasers.



Anish K. Goyal is the vice president for technology at Block Engineering, which is a manufacturer of quantum-cascade laser (QCL) and Fourier transform infrared-based infrared spectroscopy solutions. At Block Engineering, he leads all aspects of technology development, assessment, and demonstration of new commercial and government

applications, and the establishment of corporate technology strategies. He holds a doctoral degree in electrical and computer engineering from the University of California, Santa Barbara, specializing in solid-state device technology, and a bachelor's degree in electrical and computer engineering from Rensselaer Polytechnic Institute. He joined Block from Lincoln Laboratory, where he was a member of

the technical staff in the Laser Technology and Applications Group. Current areas of interest include QCL technology, standoff chemical detection, and hyperspectral imaging. He has served as an associate editor for the *IEEE Journal of Quantum Electronics* and has more than 30 publications and four patents.



Kevin J. Creedon is an associate staff member in the Laser Technology and Applications Group at Lincoln Laboratory. Since 2008, he has developed high-brightness laser sources for various applications by beam combining. He is currently working to implement coherent combining architectures using quantum-cascade lasers and pulsed fiber amplifiers.



Juliet T. Gopinath received a bachelor's degree in electrical engineering in 1998 from the University of Minnesota. She was awarded master's (2000) and doctoral (2005) degrees in electrical engineering and computer science from the Massachusetts Institute of Technology. From 2005 to 2009, she worked as a member of the technical staff at Lincoln Laboratory. Her work included wavelength beam combining of eyesafe diode arrays, cryogenic Yb:YAG lasers/amplifiers, mode-locked semiconductor optical waveguide lasers (SCOWL), high-power eyesafe laser sources, and Raman spectroscopy. She is now an assistant professor at the University of Colorado–Boulder in the Electrical, Computer, and Energy Engineering Department. Her research interests include ultrafast solid-state and fiber lasers, semiconductor lasers, wavelength beam combining, spectroscopy, nonlinear processes in fibers, mid-infrared sources, and adaptive optics. Dr. Gopinath is the recipient of the National Science Foundation Graduate Fellowship (1998–2001) and an R&D 100 Award (2012). She has authored and coauthored 29 journal papers and more than 37 conference proceedings.



Vincenzo Daneu was a staff member in the Quantum Electronics Group at Lincoln Laboratory until his retirement in 2002. He worked on solid-state and semiconductor laser development. He contributed to the development of laser sources for the generation of a sodium guide star. He performed one of the early demonstrations of wavelength beam combining using a 2 μm semiconductor laser array. He also contributed to the development of sensing technology for early warning of a biological attack. Since his retirement, he has resumed work at Lincoln Laboratory as a consultant with DAG Consulting. His recent activity has mainly been in the area of optical design and measurements. He holds a doctorate in electrical engineering from the University of Palermo, Italy.



Bien Chann was previously a technical staff member at Lincoln Laboratory, where his research interests covered wavelength beam combining (WBC), coherent beam combining, high-power laser systems, ultrafast lasers, and laser cooling. The TeraDrive™ technology is based on his work. He has published extensively in the fields of atomic physics and high-power lasers, including 16 papers in peer-reviewed journals. Dr. Chann also holds six patents issued or pending in the areas of stabilized diode arrays and stacks, single-frequency diode arrays, WBC of diode stacks, WBC of diode stacks independent of imperfections, 2D WBC laser system for scaling to the MW-power level, and multi-kW beam-combinable fiber amplifiers. Dr. Chann holds a doctorate in atomic physics from the University of Wisconsin and a bachelor's degree in physics and mathematics from Stony Brook University. Dr. Chann was a 2012 R&D 100 award winner for his work on the wavelength beam-combined diode laser. He won the 2012 Berthold Leibinger Innovationspreis (First Prize) for his work with “Dense Wavelength Multiplexing of High-Power Diode Lasers,” and was honored with the Museum of Science “Invented Here” award for his work with wavelength beam combining.



Robin Huang is a cofounder of TeraDiode and a member of its board of directors. He is responsible for business development for the government market and contributes to internal R&D and new innovations. Prior to joining TeraDiode in October 2009, Dr. Huang was a technical staff member at Lincoln Laboratory. He investigated and led Department of Defense programs on electro-optical materials and devices for high-power semiconductor lasers, thermophotovoltaic devices, mid-infrared diode lasers, quantum-cascade lasers, and vertical-cavity surface-emitting lasers. He has published over 45 papers and presented research at more than 35 conferences. Dr. Huang also has five issued U.S. patents. He holds a doctorate in applied physics and a master's degree in electrical engineering from Stanford University, and a bachelor's degree in physics with electrical engineering from the Massachusetts Institute of Technology, where he graduated Phi Beta Kappa.